Journal of Materials Chemistry A

Sustainable Seaweed-based One-dimensional (1D) Nanofibers as High-performance Electrocatalysts for Fuel Cells

Journal:	*Journal of Materials Chemistry A*
Manuscript ID:	TA-ART-05-2015-003199.R1
Article Type:	Paper
Date Submitted by the Author:	27-May-2015

Complete List of Authors:	Zhao, Wei; Qingdao University, Yuan, Pei; China University of Petroleum, State Key Laboratory of Heavy Oil Processing She, Xilin; Qingdao University, College of Chemical Engineering xia, yanzhi; Qingdao University, College of Chemical and Environmental Engineering Komarneni, Sridhar; Penn State College of Agricultural Sciences, Dept. of Crop and Soil Sciences Xi, Kai; University of Cambridge, Department of Materials Science and Metallurgy Che, Yanke; Institute of Chemistry, Chinese Academy of Sciences, ; Yao, Xiangdong; Griffith University, Queensland Micro and Nanotechnology Centre Yang, Dongjiang; Qingdao University, College of Chemical and Environmental Engineering

Journal Name

RSCPublishing

PAPER

Sustainable Seaweed-based One-dimensional (1D) Nanofibers as High-performance Electrocatalysts for Fuel Cells

0Cite this: DOI: 10.1039/x0xx00000x

Received 00th January 2012,
Accepted 00th January 2012

DOI: 10.1039/x0xx00000x

www.rsc.org/

Wei Zhao[a,b], Pei Yuan[c], Xilin She [a], Yanzhi Xia*, [a], Sridhar Komarneni[e], Kai Xi[f], Yanke Che[g], Xiangdong Yao*,[d], and Dongjiang Yang*,[a,d]

A high-performance one-dimensional (1D) nanofibrillar N-Co-C oxygen reduction reaction (ORR) catalyst was fabricated via electrospinning using renewable natural alginate and multiwalled carbon nanotubes (MWCNTs) as precursors, where Co nanoparticles (NPs) are encapsulated by nitrogen (N)-doped amorphous carbon and assembled on MWCNTs. The 1D morphology not only prevents the aggregation of the Co NPs, but also providestypical multimodal mesoporous structure which is beneficial for the O_2 diffusion and the migration of adsorbed superoxide.In combination with the high conductivity of the CNTs, the N-doped amorphous carbon shell can exert electron releasing on the encapsulated Co NPs, and thus enhance the ORR activity. It is also a protective layer to stablize the Co NPs, which ensures the catalysts a high ORR activity in both alkaline and acid medium and long-term durability. So compared with a commercial Pt/C catalyst, as expected, the N-Co-C nanofiber reported herein exhibited comparable current density and onset potential (-0.06 V), with better durability in alkaline and acid solutions and better resistance to crossover effects in the ORR.

1 Introduction

The vast amounts of biomass growing in the world's oceans offer tremendous potential for numerous uses, including as a renewable source of energy. For instance, seaweeds are excellent precursors of nanotextured carbons because their cell walls are mainly composed of a fibrillar cellulose network and an alginate mucilage.[1] More interestingly, alginate mucilage is an anionic polysaccharide that easily forms a viscous gum upon binding with water.[2,3] The negatively charged framework (-COO-) of the alginate polymers enables the simple formation of metal alginates (M-alginates) through the absorption of cations such as Co^{2+}, Cu^{2+}, Fe^{3+}, and Ni^{3+} via an ion-exchange process.[4,5] Carbonization of the M-alginates is expected to form metal (oxide) NPs encapsulated by carbon. One potential application of the carbon encapsulated metal (oxide) NPs is as a catalyst to drive oxygen reduction reactions (ORRs) in low-temperature polymer electrolyte fuel cells (PEFCs), to substitute for expensive Pt-based catalysts.[6-8] Recently, an N-M-C nanocomposite system comprising nitrogen, transition metals (oxides), particularly Co or Fe, and carbon has attracted much attention because of its high ORR performance.[9-12] Despite significant progress in non-precious-metal N-M-C ORR catalysts, only a few of these ORR catalysts can approach the efficiency of Pt-based catalysts.[9,13]

It is known thatone-dimensional (1D) nanofibers are expected to improve the durability of the catalytic NPs since the activity of the NPs cannot change much with the aspect ratio of the support.[14] Besides, the 1D supports can improve mass transport or water management due to the abundant large interconnected voids among the nanofibers. In this work, electrospun N-Co-C nanofibers (N-CACNT-NF) were prepared using sodium alginate (SA) and multiwalled carbon nanotubes (MWCNTs) as precursors. We demonstrated, as expected, that the resulting N-CACNT-NF catalyst exhibited ORR performance comparable with that of Pt/C with respect to onset potential and number of electrons transferred per O_2molecule. Notably, the N-CACNT-NF catalyst displays a comparable half-wave potential and current density, better durability in both alkaline and acid environments and better methanol tolerance than the commercial Pt/C catalyst.

2 Experimental

2.1 Materials

Metal source as $CoCl_2$ (99 wt%), ethanol (99.7 wt%) and dimethyl formamide (99 wt%) were purchased from Sinopharm Chemical Reagent Co., Ltd., Triton X-100™ (biochemical grade) and PEO (Mw = 900 kDa) were purchased from Aladdin. Sodium alginate (SA) was purchased from Alg company with Mw = 379 kDa.

Multiwall carbon nanotubes (MWCNT) were purchased from Shandong Dazhan Nano Materials Company. Ammonia and Nitrogen gases were supplied in cylinders by Heli factory with 99.999% purity. Nafion® perfluorinated resin solution containing 5% Nafion® waspurchased from Sigma-Aldrich. Ultra-pure water with resistivity > 18 MΩ·cm^{-1} was used. CNTs were purchased from Shandong Dazhan Nano Materials Company.

2.2 Fabrication of Cobalt-alginate nanofibers (CACNT-NF)

For a typical procedure,[15] solutions were prepared by making separate solutions of 3 wt% PEO and 3 wt% sodium alginate in ultra-pure water. Then combine the alginate with PEO to form a 50mL solution and the weight ratio of alginate to PEO is 7:2. Solution containing 1.0 wt% of Triton X-100™ and 5wt% of dimethyl formamide were mixed with alginate/PEO solutions. After that 175 mg carbon nanotube was added into the solution. The resultant solution was stirred for 6 h at room temperature. The electrospinning process used in this study is similar to that reported previously. A high voltage power supply (Dongwen High Voltage, China) was employed to generate the electric field of 0-30 kV and the applied voltage was fixed at 20 kV in this study.[16] The typical distance between the syringe tip and the collector was 20 cm. The outer diameter of the syringe tip was 0.7 mm and the flow rate is 0.5 mL/h. After 6 hours of electrospinning, the SA fibrous membranes were dried in a vacuum oven at a temperature of 50 °C overnight to dry off any remaining solvent. Then the SA nanofibers were immersed in $CoCl_2$ (0.5 mol/L) alcohol solution to form the CACNT-NF.

2.3 Preparation of the N-CACNT-NF electrocatalysts

The obtained CACNT-NF were weighted and placed in a tube furnace. Then they were heated from room temperature at a heating rate of 1 °C/min to 180 °C where they were treated for 2 h in air. The as-stabilized nanofibers were subsequently heated to 600 °C at the heating rate of 2 °C/min in nitrogen/ammonia (v/v=1:1) mixed gas. After reaching the specified temperature, the nanofibers were treated for another 1 h in nitrogen/ammonia (v/v=1:1) mixed gas with the flow rate of 80 ml/min to form the N-CACNT-NF electrocatalysts.

2.4 Characterizations

The morphology and structure of the N-CACNT-NF nanofibres were investigated by field emission scanning electron microscopy (FESEM; JSM-7001F, JEOL, Tokyo, Japan). The phase structures were characterized with X-ray diffraction (XRD, DX2700, China) operating with Cu Kα radiation (l = 1.5418 Å) at a scan rate (2θ) of 2° min^{-1} with the accelerating voltage of 40 kV and the applied current of 30 mA, ranging from 10 to 80 °.Specific surface area was calculated by the Brunauer-Emmett-Teller (BET) method from the data in a relative pressure (P/P_0) range between 0.05 and 0.20, pore size distribution plots were derived from the adsorption branch of the isotherms based on the BJH model. Raman spectrometer (Renishaw, inVia) was used to acquire the Raman spectra. TEM and high-resolution TEM (HRTEM) images were obtained using a FEI Tecnai 20 TEM with an accelerating voltage of 200 kV. The chemical composition was investigated by X-ray photoelectron spectroscopy (XPS) using an ESCALab250 electron spectrometer (Thermo Scientific Corporation) with monochromatic 150 W Al Kα radiation. Thermogravimetric analysis (TGA) measurement was carried out on an EXSTAR TG/DTA 6300 instrument (Seiko Instruments, Japan), the N-CACNT-NF nanofibres were heated to 900°C with a heating rate of 10 °C min^{-1} in air.

2.4 Electrochemical Measurements

The electrocatalytic activity of N-CACNT-NF catalysts is measured in a solution of 0.1 M KOH using cyclic voltammetry at room temperature. An ink of the catalyst was prepared by mixing 2 mg of catalyst powder with 20 μL of a 5wt % Nafion solution/350μL of ethanol and placed in an ultrasonic bath. After that a drop of the ink was pipetted onto a glassy carbon disk (0.0706 cm^2). Measurements were performed in a three-electrode, one-compartment cell at room, equipped with a Pt wire counter electrode and a Ag/AgCl reference electrode. Cyclic voltammograms with a sweep rate of 100mv/s are recorded in the potential range of 0 to -1.2 V versus a Ag/Ag Clreference electrode. Linear sweep voltammetry (LSV) was performed in N_2-saturated or O_2-saturated 0.1 M KOH. ORR current-voltage curves were recorded at a scan rate of 10 mV/s under various electrode rotation rates (625, 900, 1025, 1600, 2025, 2600 rpm respectively).

RDE test in acidic mediawas conducted using a saturated calomel electrode (SCE, SCE was converted to RHE using the following relationship. E(RHE) = E(SCE) + 0.244 V + 0.059 × pH) as the reference electrode and a platinum rod as the counter electrode. Before the start of each measurement, 1 M $HClO_4$ electrolyte was bubbled with O_2 for > 30 min. The relative ORR cathodic stability performance (1600 rpm) of the N-CACNT-NF catalysts was measured at a scan rate of 10 mV s^{-1} in O_2-saturated 1 M $HClO_4$ electrolyte before and after adding 0.4 mMH_2O_2.

RRDE test in alkaline mediawas conducted using a Ag/AgCl as the reference electrode and a platinum rod as the counter electrode. Before the start of each measurement, 0.1 M KOH electrolyte was bubbled with O_2 for > 30 min. The RRDEmeasurements were carried out at 1600 rpm using a CHI 760E workstation (CH Instruments, Inc.) with a RRDE-3A rotator (ALS Co., Ltd).

The electron transfer number (n) was determined from RRDE measurement on the basis of the diskcurrent (I_D) and ring current (I_R) via the following equation:

$$n=4\ I_D/(I_D+I_R/N);$$

The peroxide percentage (H_2O_2 %) was calculated based on the following equation:

$$H_2O_2\ \%=200\ I_R/N/(I_D+I_R/N);$$

Where N=0.43 is the current collection efficiency of Pt ring.

3 Results and discussion

As illustrated in Scheme 1a, we obtained a grey, non-woven web composed of SA/CNTs nanofibers (SACNT-NF) via electrospinning,

and single SACNT-NF exhibited a smooth, bead-free surface, indicating that the CNTs and the SA molecules mixed well in the nanofibers. After the SACNT-NF web was immersed in an aqueous solution of $CoCl_2$ (0.5 mol/L), the grey nanofibrillar web was converted into a purple web (Scheme 1b-c and Figure S1). In this step, the G segments of the alginate framework were apparently aligned side-by-side to form an "egg-box" structure in which the Co^{2+} ions were confined by coordination with the polymer chains.[17,18] The diffraction peak at 21.0° is detected from the powder XRD pattern of CACNT-NF (Figure S2). This peak is ascribed to the (002) plane of Co-alginate, which is from the layer spacing along the molecular chain direction, and indicates the formation of "egg-box" structure.[17, 19] The SACNT-NF were then converted into Co-alginate/CNT nanofibers (CACNT-NF). The nanofibrillar N-Co-C non-woven web was formed after the carbonization of CACNT-NF under NH_3 atmosphere. As shown in the SEM image in Scheme 1d, the diameter of the N-doped CACNT-NF (N-CACNT-NF) ranged from 60 to 100 nm and was much smaller than those of the SACNT-NF and CACNT-NF, which were in the range of 150-200 nm. We attributed this decrease in diameter of the N-doped CACNT-NF to the release of H_2O and CO_2 during the thermal decomposition of the alginate. Additionally, a rough surface was observed for the N-CACNT-NF on which numerous beads (30-40 nm) were distributed homogeneously.

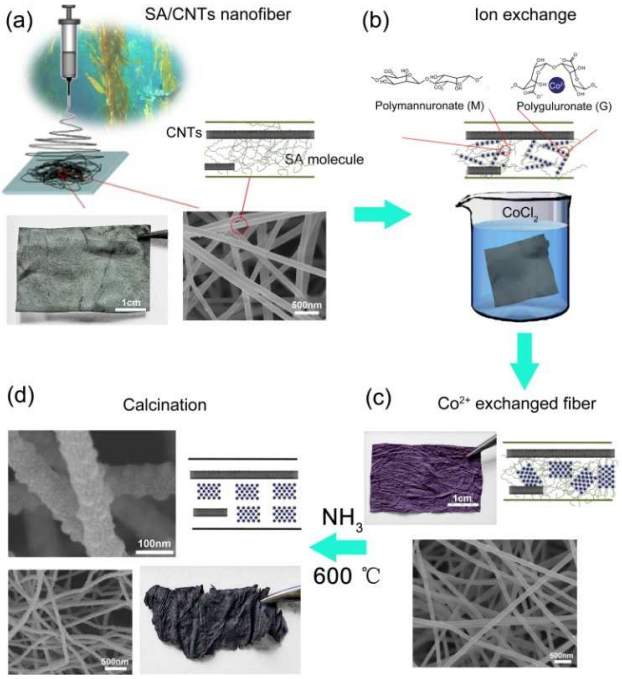

Scheme 1 Procedure for fabrication of the electrospun N-Co-C nanofibres in the presence of SA and MWCNTs as precursors.

The XRD pattern of N-CACNT-NF shows that the Co^{2+} ions were fully converted into Co metal (Figure 1a) during the carbonization process. The diffraction peaks of the CNTs were also detected from the pattern, indicating the CNTs were doped into the nanofibers. As is shown in Figure 1b, Raman spectroscopy is used to characterize the structural difference between N-CACNT-NF, N-CA-NF(the N-doped electrospun Co-alginate nanofibers) and C-CACNT-NF(the carbonized electrospun CACNT-NF in N_2 atmosphere). It is found that N-CA-NF has two weak peaks at 1338 cm^{-1} (D band) and 1594 cm^{-1} (G band). The G band is represents sp^2 carbon atoms domains while the D band reveals the sp^3 defects within the structure. The N-CACNT-NF has three typical peaks, the D band at 1327 cm^{-1}, the G band at 1600 cm^{-1} and the 2D band at 2670 cm^{-1}. Both the D band and G band of N-CACNT-NF and C-CACNT-NF are stronger than that of N-CA-NF due to the addition of CNTs. The relative lower I_D/I_G value (0.926) of N-CA-NF indicates more graphitic domains, while the higher I_D/I_G value (1.21) of N-CACNT-NF reveals a better catalytic activity of the ORR because of the increased active sites provided by much defects on N-CACNT-NF.[20]

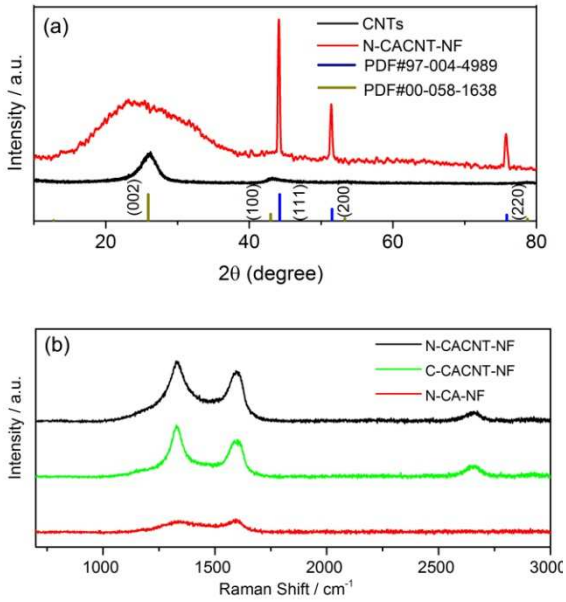

Fig. 1 (a) XRD patterns of N-CACNT-NF. (b) Raman spectra of N-CACNT-NF, C-CACNT-NF and N-CA-NF

The BET (Brunauer–Emmett–Teller) surface area and single-point total pore volume of the N-CACNT-NF were 173 m^2 g^{-1} and 0.65 cm^3 g^{-1}, respectively (Figure 2a); these results were apparently due, in part, to the presence of CNTs in the nanofibers. As shown in Figure 2b, the average Barrett–Joyner–Halenda (BJH) pore diameter calculated from the desorption branch of the isotherm was mainly centered at ~37 nm, in addition to a weak distribution determined at ~2.6 nm. We attributed the multimodal porosity of the sample to the connected internanofiber voids (~37 nm) and vacancies (~2.6 nm) that remained after the release of H_2O and CO_2 during the thermal decomposition of the alginate.[21] In contrast, the pore size of conventional porous carbon-based ORR catalysts is usually less than 10 nm, which is too narrow for efficient transport and accessof the proton-exchange ionomers because of the sluggish reaction kinetics of the ORR.[22] Here, the large mesoporous internanofiber voids are expected to facilitate the diffusion of reactants during the ORR

process, since large-sized mesopores are very effective for acceleration of the ORR.[23]

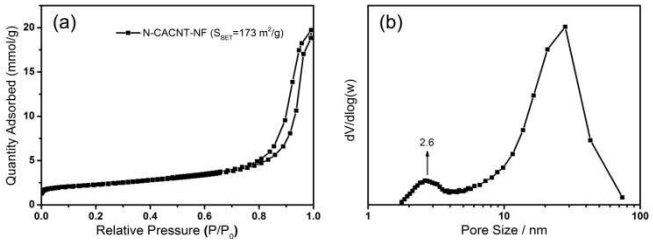

Fig. 2 (a) N_2 adsorption-desorption isotherm of N-CACNT-NF. (b)The pore size distribution of N-CACNT-NF.

Figure 3a shows a typical transmission electron microscopy (TEM) image of N-CACNT-NF. It revealed that the nanofibers were composed of MWCNTs (Figure 3b), amorphous carbon, and Co NPs, which tangled together to form the 1D nanostructure (upper right inset in Figure 3a). The 1D morphology can avoidthe aggregation of the Co NPs and improve their durability. The diffraction spots in the inset electron diffraction pattern (EDP) were indexed as the (210), (110), and (111) planes of the Co NPs. The high-resolution TEM (HRTEM) image shows a set of lattice fringes with a spacing of 0.25 nm, corresponding to the (111) plane of Co NPs(Figure 3e). The size distribution of Co NPsis estimated from the HRTEM images and the average size of Co NPs is approximately 17 nm(Figure 3c).The content of Co in a single N-CACNT-NFis 22.79% by weight(Figure S3). These Co NPs are encapsulated by amorphous carbon resulted from the carbonization of the alginate "egg-box". In comparison with edge-doped CNTs, the defect-rich amorphous carbon is easier to be doped by nitrogen atoms.Elemental mapping analysisindicates the presence of Co, C, and O components in a single N-CACNT-NF (Figure 3d).

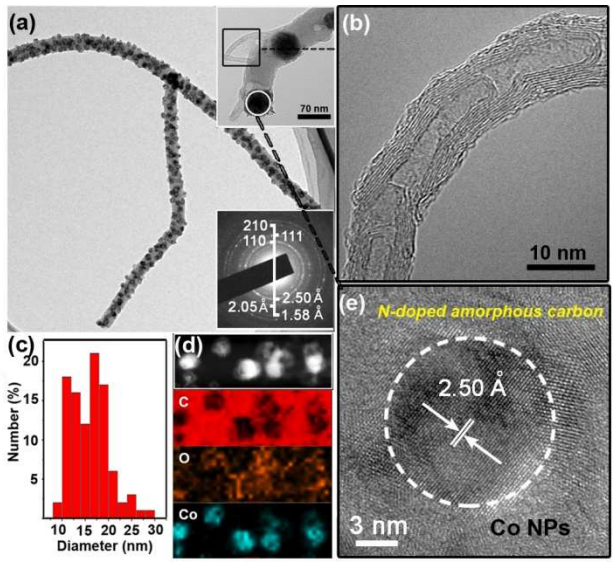

Fig.3 (a) TEM image of N-CACNT-NF. Insets: EDP of the Co NPs in the nanofiber (the bottom right); amplified TEM image of a single N-CACNT-NF. (b, e) HRTEM image of the CNT and Co NPs in the N-CACNT-NF. (c) Size distribution of Co NPs estimated from the HRTEM images.(d) EDS elemental mapping images (C, O, and Co) of a single N-CACNT-NF.

The doped N atoms can be revealed by the X-ray photoelectron spectroscopy (XPS) (see Figure 4c and S4), and ca. 1.9wt % nitrogen was doped in the nanofibers. Pyridinic-N and pyrrolic-N were observed at 398.5 and 400.0 eV, respectively.[10, 24] Both of them can exert electron releasing on the encapsulated Co NPs, and are believed to play a significant role in improving the electrocatalytic activity toward the ORR. The high-resolution C1s spectrum revealed three states of carbon in the material (Figure 4a). The emergence of the peaks at 286.0 and 288.6 eV was attributed to C–O and C=O coordinations, respectively,[25] which stemmed from the pyrolysis of CA. Another peak at 284.6 eV was assigned to the graphitic carbon of the CNTs.[26] The deconvoluted XPS O1s spectrum of the N-CACNT-NF is shown in Figure 4b. The peaks at 531.2 and 533.0 eV were assigned to C-OH coordination and C-O-C coordination, respectively, and the strong peak at 530.0 eV was attributed to metal-oxide residues and C=O coordination.[27]The deconvoluted XPS N1s spectrum (Figure 4c) displays six signals at 398.5, 399.4, 400.0, 401.2, 402.4 and 403.7 eV. The peak at 398.5 eV was ascribed to pyridinic N, and the peak at 400.0 eV was assigned to pyrrolic N. The other peaks, at 401.2, 402.4 and 403.7 eV, were mainly owing to azide units.[10] The pyridinic-N and pyrrolic-N can exert electron releasing on the encapsulated CoNPs, and are believed to play a significant role in improving the electrocatalytic activity toward the ORR.

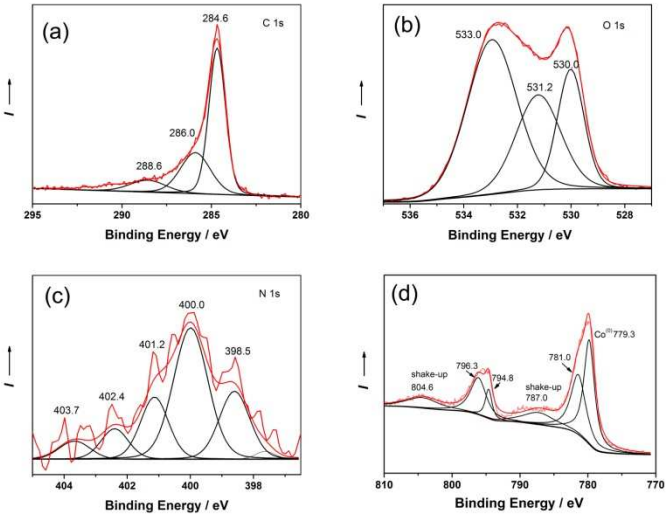

Fig. 4 The deconvoluted XPS spectra for N-CACNT-NF: (a) C1s , (b) O1s, (c) N1s, and(d) Co2p spectra.

The deconvoluted XPS Co 2p spectrum is displayed in Fig. 4d. The firstmain peak at ~779.3 eV was assigned to Co $2p_{3/2}$ binding energy of Co in a zerovalent state.[28] The peak at ~781.0 eV can be attributed to cobalt oxides.[29] The existence of cobalt oxides showed that the Co NPs on the surface of N-CACNT-NF were oxidized in the air for the fact that $Co^{(0)}$ is sensitive to aerobic atmosphere.[30] The

peak at ~796.3 eV was ascribed to the Co $2p_{1/2}$ states. Pyridinic N might improve the onset potential for ORR by converting the ORR reaction mechanism from a $2e^-$ dominatedprocess to a $4e^-$ dominated process. Those N-doped sites can activate the Faradic process,[31] while Cometal-ion centers have been found to display the optimal electrocatalytic properties, attributed to their distinct redox propertiesand have also been proposed as the active site for the ORR.[32]

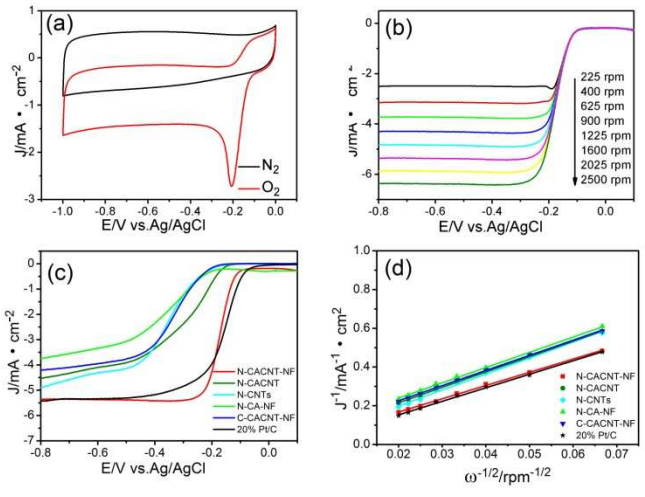

Fig.5(a) CV curves obtained from N-CACNT-NF in N_2- and O_2-saturated 0.1 M KOH. (b) RDE curves of N-CACNT-NF, N-CACNT, N-CNTs, N-CA-NF, C-CACNT-NF and 20% Pt/C. (c) LSV curves obtained for N-CACNT-NF at various rotation speeds; (d) K-L plots for these samples obtained from the LSV curves obtained at –0.6 V in (c) and Figure S6.

The N-CACNT-NF catalyst was examined by cyclic voltammetry (CV) in N_2- or O_2-saturated 0.1 M KOH aqueous solution at a scan rate of 100 mV s^{-1}. As shown in Figure 5a, a voltammogram with no significant peaks was obtained in the N_2-saturated solution. However, a well-defined reduction peak occurred at approximately –0.21 V (vs. Ag/AgCl) in the O_2-saturated solution, indicating that O_2 was reduced on the electrode coated with the N-CACNT-NF catalyst with a very positive potential. This value is much more positive than those of the N-doped electrospun Co-alginate nanofibers (N-CA-NF), the N-doped MWCNTs (N-CNTs), the carbonized electrospun CACNT-NF in N_2 atmosphere (C-CACNT-NF), and the N-doped physical mixture of Co-alginate and MWCNTs (N-CACNTs) as electrodes (see Figure S5). In addition, linear sweep voltammetry (LSV) was performed on a rotating disk electrode (RDE) in O_2-saturated 0.1 M KOH at 1600 rpm. As shown in Figure 5c, the ORR onset potential of the N-CACNT-NF catalyst is –0.06 V, which is very similar to that of the highly active commercial Pt/C electrode (–0.03 V) and is much more positive than those of N-CA-NF, N-CNTs, C-CACNT-NF, and N-CACNTs. The N-CACNT-NF catalyst also exhibited a half-wave potential ($E_{1/2}$) of –0.168 V, which is comparable to that of the Pt/C (–0.154 V) and much more positive than those of the other samples. Moreover, the highest current density was achieved with N-CACNT-NF, followed by C-CACNT-NF, N-CACNTs, N-CNTs, and N-CA-NF, because the electrospun nanofibers incorporated the merits of the highly conductive CNT component and the 1D morphology.

Furthermore, the number of transferred electrons per O_2 (n) involved in the ORR of the N-CACNT-NF catalyst was calculated using the Koutecky-Levich (K-L) equation.[26, 33] As illustrated in Figure 5b, a series of LSV curves for N-CACNT-NF were recorded on an RDE rotating at speeds from 400 to 2600 rpm. The value of *n* at different potentials was determined using the K-L plots in Figure 5d and Figure S6. All of the plots show good linearity at different rotation speeds, and the calculated *n* of the N-CACNT-NF is 3.98 at –0.6 V, indicating that the N-CACNT-NF catalyst proceeds mainly through a four-electron mechanism. In contrast, the n values of N-CACNT, N-CNTs, N-CA-NF, C-CACNT-NF electrodes are 3.54, 3.33, 3.53, and 3.59, respectively (see Figure S7). The Tafel slopes of N-CACNT-NF and Pt/C were derived from the linear plots of the LSVs at 1600 rpm (Figure S8). In the low-overpotential region, where the overall ORR speed is determined by the surface reaction rate on the catalyst,[34] the Tafel slope of the N-CACNT-NF (52 mV dec^{-1}) was very similar to that of Pt/C (55 mV dec^{-1}), indicating that N-CACNT-NF possessed an *n* value comparable with that of Pt/C. However, in the high-overpotential region, where the overall ORR rate is dependent on the mass transfer, the Tafel slope value of the N-CACNT-NF (110 mV dec^{-1}) was much smaller than that of Pt/C (120 mV dec^{-1}), suggesting much smoother reactant diffusion through the large voids of the 1D nanofiber catalyst. We also calculated the kinetic limiting current (J_k) from the intercept of the linearly fitted K-L plots at –0.6 V (Figure S7), and determined that the J_k value of N-CACNT-NF is greatly superior to those of other catalysts.

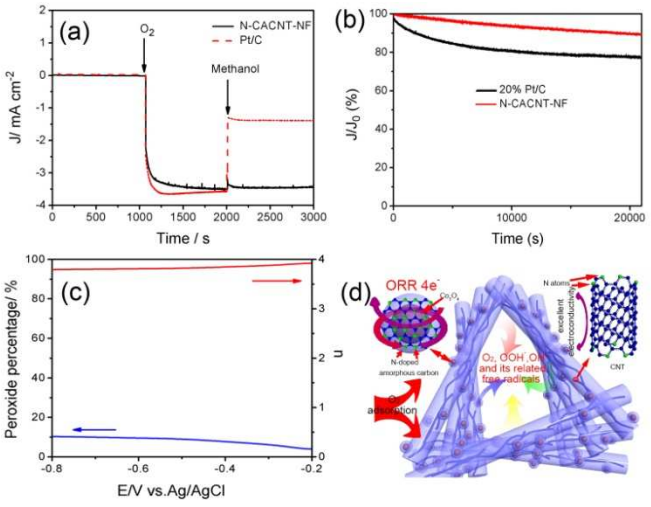

Fig. 6 (a) Methanol crossover resistance (at –0.27 V vs. Ag/AgCl) and (b) Long-term stability (–0.6 V vs. Ag/AgCl) test of N-CACNT-NF and 20% Pt/C in 0.1 M KOH. (c) H_2O_2 yield plots (blue line) and electron-transfer number (red line) of N-CACNT-NF in 0.1 M KOH. (d) The proposed synergetic mechanism of N-CACNT-NF in ORR process.

The tolerance of N-CACNT-NF and Pt/C to the crossover effect was evaluated and shown in Figure 6a. A negative current appeared when O_2 was introduced into the N_2-saturated KOH solution at 1000 s. The current of Pt/C instantaneously increased to more positive values when 20% methanol was added to the O_2-saturated KOH solution at 2000 s. However, the current of the N-CACNT-NF remained stable, showing remarkably better tolerance to methanol crossover than the commercial Pt/C catalyst. Furthermore, the stability of the N-CACNT-NF was tested at −0.60 V for 20000s. Apparently, the corresponding current-time (i-t) chronoamperometric response of the N-CACNT-NF exhibited a slow attenuation and a high relative current of 91 % that persisted after 20000s (see Figure 6b). This relative current value is higher than that of the Pt/C catalyst (75%), indicating high durability in alkaline medium. The low durability of Pt/C is caused by the aggregation of Pt nanoparticles,[35] while the Co NPs of N-CACNT-NFavoid this kind of aggregation for encapsulated by amorphous carbon and nanofiber structure. Compared with the i-t chronoamperometric response of N-CACNT(Figure S9), N-CACNT-NF shows a better stability of active reaction sites. 1D morphology improves the durability for the Co NPs cannot change much with the aspect ratio of the support. Similarly, the N-CACNT-NF also exhibited the good electrochemical activity for ORR and the superior stability in $H_2O_2/HClO_4$ system (see Figure S10).The selectivity of the four-electron reduction of oxygen for N-CACNT-NF was further studied using the RRDE technique (see Figure 6c and Figure S11). The H_2O_2 yield of as-prepared N-CACNT-NFcatalysts remained below 10.13% at all potentials, corresponding to a high electro-transfer number of 3.89, which is in accordance with the K-L plots results.

We proposed a synergetic mechanism to explain the superior ORR performance of the nanofibrillar catalyst. As presented in Figure 6d, the abundant pyridinic-N and pyrrolic-N in the amorphous carbon capsule layer on the Co NPs could exert electron releasing on the encapsulated Co NPs and thus enhance their ORR activity.[36] The amorphous carbon layer also acts as a protective layer to stabilize the Co NPs, which ensures the Co NPs could display good ORR performance and long-term durability in both alkaline and acid solution. In addition, the 1D morphology of the nanofiber is also crucial for the enhancement of ORR activity. For instance, its unique large voids (~37 nm) upon entangled piling of 1D nanofibers facilitate the O_2 diffusion and the migration of adsorbed superoxide which is a rate determining step for the whole reaction.[37] The small mesopores on the surface of the nanofibers (~2.6 nm) are favourable for the adsorption of O_2 molecules. Finally, the excellent electrical conductivity of the MWCNTs entangled in the nanofibers is helpful for a fast and smooth electron transfer in ORR process.

4 Conclusions

In summary, this work reports the development of high-performance ORR catalysts using renewable seaweed biomass, which simultaneously features three advantages: 1) Natural SA is a renewable and inexpensive carbon precursor in which Co species are more easily deposited via a facile ion-exchange process compared to conventional Co macrocycle compound precursors; 2) The active Co NPs are encapsulated by N-doped amorphous carbon which can not only exert electron releasing on the encapsulated Co NPs, but also act as a protective layer to stabilize the Co NPs; 3) The 1D morphology prevents the aggregation of the Co NPs, and the large interconnected voids (several dozens of nanometers in size) among the nanofibers are a unique structural feature of the electrospun nanofibers, which facilitates mass and electron transport for ORR electrodes.

Acknowledgements

This work was financially supported the National Natural Science Foundation of China (No. 51473081 and 21207073), ARC Discovery Project (Grant no.130104759), “Youth 1000 Talent Plan” Fund, and State Key Lab of Multiphase Flow in Power Engineering for financial support.

Notes and references

[a]State Key Laboratory Cultivating Base of Advanced Fibres and Textile Materials, Qingdao University, Qingdao, Shandong 266071,China.E-mail: d.yang@qdu.edu.cn; xiayzh@qdu.edu.cn.

[b]National Engineering Laboratory for Modern Silk, College of Textile and Clothing Engineering, Soochow University, Suzhou, Jiangsu 215123, Chi na.

[c]State Key Laboratory of Heavy Oil Processing, China University of Petroleum, Beijing 102249, China.

[d]Queensland Micro- and Nanotechnology Centre (QMNC) Griffith UniversityNathan, Brisbane, QLD 4111, Australia. Email: x.yao@griffith.edu.au

[e].Materials Research Institute and Department of Ecosystem Science and Management, The Pennsylvania State University, University Park, PA16802, USA.

[f]Department of Materials Science and MetallurgyUniversity of Cambridge, Cambridge, UK.

[g]Institute of Chemistry,The Chinese Academy of Sciences, Beijing, P R China.

**W. Zhao and P. Yuan contributed equally to this work.

†Electronic Supplementary Information (ESI) available: Experimental details and extra information on structural and electrocatalytic activity analysis. See DOI: 10.1039/c000000x/

1. T.Helgerud, O.Gåserød,T. Fjæreide, P. O. Andersen, C. K. Larsen, *Food Stabilisers, Thickeners and Gelling Agents,*(Eds: A. Imeson), Wiley-Blackwell,2009, pp. 50-72.
2. B. H. A.Rehm, *Biopolymers Online*, *Alginates from Bacteria*, Wiley-VCH, Verlag GmbH & Co. KGaA, 2005.
3. P. E.Raymundo, M.Cadek, F. Beguin, *Adv. Funct. Mater.,*2009, **19**, 1032-1039.
4. P. Agulhon, V. Markova, M. Robitzer, F. Quignard, T. Mineva, *Biomacromolecules,*2012,**13**, 1899-1907.
5. A. Haug, B. Larsen, O. Smidsrod, *Acta. Chem. Scand.,*1967, **21**, 691.
6. R. Bashyam, P. Zelenay, *Nature,*2006, **443**, 63-66.
7. J. Greeley, I. E. L. Stephens, A. S. Bondarenko,T. P. Johansson, H. A. Hansen, T. F. Jaramillo, J. Rossmeisl, I. Chorkendorff, J. K. Nørskov, *Nature Chem.,*2009, **1**, 552-556.
8. F. Jaouen, E. Proietti, M.Lefèvre, R. Chenitz, J. P. Dodelet, G. Wu, H. T. Chung, C. M.Johnstonb, P.Zelenay,*Energy Environ. Sci.,*2011, **4**, 114-130.

9. G. Wu, K. L. More, C. M. Johnston, P. Zelenay, *Science,*2011, **332**, 443-447.
10. Z. S. Wu, S. Yang, Y. Sun, K. Parvez, X. Feng, K. Müllen, *J. Am. Chem. Soc.,*2012,**134**, 9082-9085.
11. M. Liu, R. Zhang, W. Chen, *Chem. Rev.,*2014, **114**, 5117-5160.
12. W. Han, L. Ren, L. Gong, X. Qi, Y. Liu, L. Yang, X. Wei, J. Zhong, *ACS Sustainable Chem. Eng.,*2014,**2**, 741-748.
13. J. Liu, X. Sun, P. Song, Y. Zhang, W. Xing, W. Xu, *Adv. Mater.,*2013, **25**, 6879-6883.
14. M. K. Debe, *Nature*, 2012, **486**, 43-51.
15. C. D. Saquing, C. Tang, B. Monian, C. A. Bonino, J. L. Manasco, E. Alsberg, S. A. Khan, *Ind. Eng. Chem. Res.* 2013, **52**, 8692-8704.
16. A. Greiner, J. H. Wendorff, *Angew. Chem. Int. Ed.* 2007, **46**, 5670-5703.
17. P. Sikorski, F. Mo, G. Skjak-brak, *Biomacromolecules,*2007, **8**, 2098-2013.
18. D. Li, D. Yang, X. Zhu, D. Jing, X. Zhi, Q. Ji, R. Cai, H. Li, Y. Che, *J. Mater. Chem. A*, 2014, **2**, 18761-18766.
19. L. Li, Y. Fang, R. Vreeker, I. Appelqvist. *Biomacromolecules*, 2007, **8**, 464-468.
20. S. Yang, X. Song, P. Zhang and L. Gao, *ACS Appl. Mater. Interfaces*, 2013, **5**, 3317–3322.
21. S. K. Meher, P. Justin, G. R. Rao, *Nanoscale,* 2011, **3**, 683-692.
22. J. Liang, Y. Zheng, J. Chen, J. Liu, D. Hulicova-Jurcakova, M. Jaroniec, S. Z. Qiao, *Angew. Chem. Int. Ed.,* 2012, **51**, 3892-3896.
23. J. Tang, J. Liu, C. Li, Y. Li, M. O. Tade, S. Dai, Y. Yamauchi, *Angew.*2015, **54**, 588–593.
24. S. Yang, X. Feng, X. Wang, K. Mullen, *Angew. Chem. Int. Ed.,* 2011, **50**, 5339-5343.
25. S. Smith, M. Jaroniec, G. Q. Lu, S. Z. Qiao, *J. Am. Chem. Soc.* 2011, **133**, 20116-20119.
26. S. Wang, D. Yu, L. Dai, D. W. Chang, *ACS Nano*, 2011, **5**, 6202-6209.
27. W. Wei, H. Liang, Parvez, K. Zhuang, X.Feng, X. Mullen, K. *Angew. Chem.* 2014, **126**, 1596-1600.
28. Y. Su, Y. Zhu, H. Jiang, J. Shen, X. Yang, W. Zou, J. Chen, C. Li, *Nanoscale*, 2014, **6**, 15080-15089.
29. M. Ibrahim, C. Marcelot-Garcia, K. A. Atmane, E. Berrichi, L. M. Lacroix, A. Zwick, B. Warot-Fonrose, S. Lachaize, P. Decorse, J. Y. Piquemal, G. Viau, *J. Phys. Chem. C*, 2013, **117**,15808-15816.
30. S. Guo, S. Zhang, L. Wu, S. Sun, *Angew. Chem. Int. Ed.*, 2012, **51**, 11770-11773.
31. T. Yang, J. Liu, R. Zhou, Z. Chen, H. Xu, S. Qiao, M, J. Monteiro, *J. Mater.Chem. A*, 2014, **2**, 18139-18146.
32. P. Vasudevan, S. N. Mann,S. Tyagi,*Transition Met. Chem.*, 1990, **15**, 81–90.
33. W. Chen, S. Chen, *Angew. Chem. Int. Ed.,*2009,**48**, 4386-4389.
34. Y. Liang, Y. Li, H. Wang, J. Zhou, J. Wang, T. Regier, H. Dai, H. *Nat. Mater.,*2011, **10**, 780-786.
35. J. Zhang, D. He, H. Su, X. Chen, M. Pan, S. Mu, *J. Mater. Chem A,* 2014, **2**, 1242-1246.
36. Z. Chen, D. Higgins, A. Yu, L. Zhang, J. Zhang, *Energy Environ. Sci.,*2011, **4**, 3167-3192.
37. X. She, D. Yang, D. Jing, F. Yuan, W. Yang, L. Guo, Y. Che, *Nanoscale*, 2014, **6**, 11057-11061.

TOC

A high-performance nanofibrillar N-Co_3O_4-C oxygen reduction reaction (ORR) catalyst was fabricated via electrospinning using renewable natural alginate and multiwalled carbon nanotubes (MWCNTs) as precursors. The overall electron transfer number for the catalyzed ORR was determined to be 3.98, indicating that the ORR process was dominated by a four-electron transfer process. Compared with a commercial Pt/C catalyst, the N-Co_3O_4-C catalyst reported herein displayed comparable current density and onset potential (-0.06 V), with better durability in alkaline and acid solutions and better resistance to crossover effects in the ORR.